



# Volcanic Ash Contamination of High Voltage Insulators

EEA Conference & Exhibition 2011, 23-24 June, Auckland

Supervisor: Professor Pat Bodger, University of Canterbury

Student, Author & Presenter: Alan Wightman, University of Canterbury

Number of Pages: 10 + Appendices

## **Abstract**

Recent work in the University of Canterbury high voltage laboratory uncovered an interesting phenomenon. While studying the effect of volcanic ash contamination on high voltage insulator flashover levels, ash was seen ‘blowing’ off the insulator surface before flashover occurred. The goal of this project was to investigate and explain the observed phenomenon to provide a basis for potential development of self-cleaning insulators.

Four different types of insulator and three different ash grain sizes were tested. The insulator electric fields were modelled; corona discharge waveforms and visual observations were obtained. Areas of ash removal coincided with areas of corona discharge. It was initially proposed that the ash was removed by an alternating current corona wind however the results do not support this theory. Instead, the observed results suggest that the ash acquires a negative charge and is removed by an electrostatic force. The electrostatic force is strongest during the negative half cycle of the applied voltage due to space charge and hence the ash pulses off the insulator at 50Hz.

The amount of ash removed increased with the applied voltage however this led to a trade off between ash removal and flashover. The maximum amount of ash removed during this project was approximately 90% from the top weather shed and 30% from the middle and bottom weather sheds. This study focused on the removal of dry ash. It is unlikely that wet ash can be removed in this fashion, without flashover, due to the conductive and adhesive nature of wet ash.

## 1. INTRODUCTION

Ash from volcanic eruptions poses a threat to power systems world-wide. Layers of ash can cover vast areas of land. Ash is highly conductive and harder to remove when wet [1], and may obtain moisture from the eruption or from rain. Ash deposited on insulators can cause flashovers, corrosion, and high leakage currents which can lead to pole fires [1].

High voltage insulators are required to provide both mechanical strength and electrical insulation. For example, insulators used on transmission lines, shown in Figure 1, suspend high voltage cables from the towers while preventing the flow of electricity between the cable and the grounded tower. If the insulator fails the high fault current which flows is a safety hazard and has the potential to damage equipment throughout the power system. Protection systems therefore automatically disconnect the faulted line from the rest of the system until the fault is removed. Blackouts may occur due to automatic disconnection of lines.

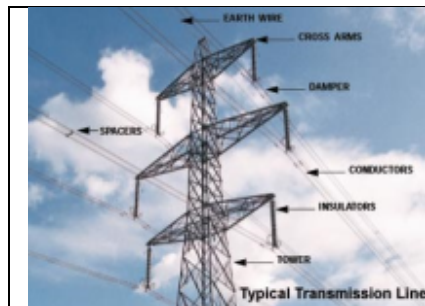


Figure 1: High voltage insulators on a transmission line.



Figure 2: Manual cleaning of an insulator after the 1995 Ruapehu eruption [2].



Figure 3: Man hitting pedestal with a hammer to loosen ash after the 1980 Mt St. Helens eruption [1].

Current methods of cleaning insulators include manual cleaning of de-energised equipment (Figure 2 and Figure 3), and water-blasting live equipment from a helicopter. These are time consuming and expensive methods. Furthermore, manual cleaning requires controlled power outages which carries the risk of further blackouts; and helicopter cleaning may not be possible following an eruption due to ash interfering with the engine [1].

Recent work in the University of Canterbury high voltage laboratory uncovered an interesting phenomenon. While studying the effect of volcanic ash contamination on high voltage insulator flashover levels, ash was seen 'blowing' off the insulator surface before flashover occurred. The goal of this project was to investigate and explain the observed phenomenon to provide a basis for potential development of self-cleaning insulators.

## 2. HYPOTHESIS

It was proposed that the phenomenon observed in the University of Canterbury high voltage lab was AC corona wind and that this wind had the potential to completely remove volcanic ash contamination from high voltage insulators.

### 3. BACKGROUND

#### 3.1 Corona Wind

The phenomenon of electric or corona wind was actively studied in the 18<sup>th</sup> and 19<sup>th</sup> centuries by the likes of Newton, Cavallo, Maxwell and Faraday [3]. Aerodynamics, heat transfer and propulsion have been areas of recent investigation for applications of corona wind. However the literature focuses on direct current corona wind, no mention of AC effects is made [3] [4] [5] [6] [7] [8].

Corona wind is the movement of air caused by strong electric fields. A strong electric field exists around high voltage insulators due to one end being connected to a high voltage line and the other end being connected to earth. In areas where the electric field is particularly strong, such as at sharp points, corona discharge may occur. Corona discharge is an ‘electron avalanche’ – it is a process where a free electron collides with an air molecule, knocking another electron free. These electrons collide with other molecules, knocking more electrons free and so on. Corona discharge causes a measurable current pulse in the line. It also causes a violet glow and audible hum. The positive ions created are repelled or attracted to the high voltage end of the insulator depending on the voltage polarity at any given instant. The ions transfer momentum to other air molecules via collisions and hence a corona wind is created [4]. The force of the wind is given by [4]:

$$F = QE \quad \text{Equation 1}$$

Where:  $F$  is the force (N)

$Q$  is the total ion charge (C)

$E$  is the electric field strength (V/m)

#### 3.2 Insulator Construction

A cap and pin ceramic insulator cross section is given in Figure 4. Glass insulators have the same construction, except use glass rather than porcelain weather sheds and typically use aluminous cement [9].

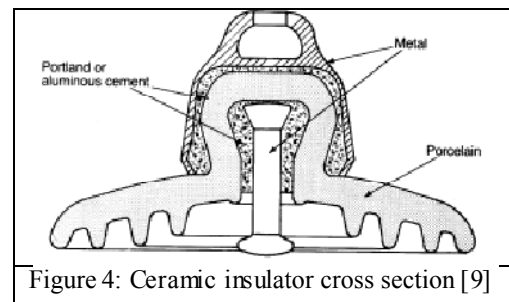


Figure 4: Ceramic insulator cross section [9]

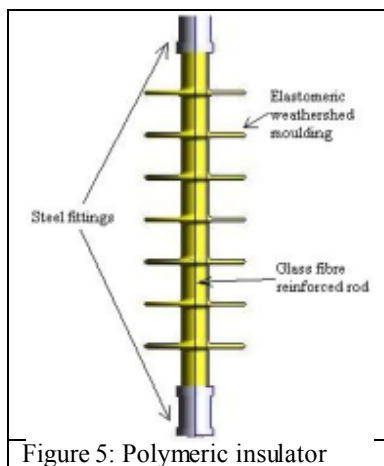


Figure 5: Polymeric insulator

Figure 5 shows a polymeric insulator which consists of a polyester or epoxy glass-fiber reinforced rod with steel fittings crimped on at each end, and with an elastomeric weather-shed mould around the rod to prevent weather and electrical discharge damage [9].

## 4. EXPERIMENTAL SET-UP

### 4.1 Corona Discharge Measurement

The set-up outlined in Figure 6 to Figure 12 allowed a voltage of up to 330kV to be applied across an insulator and the applied voltage and corona discharge measured, while working at a safe distance. The insulator was hung inside a large Perspex box to contain the ash. The top of the insulator was connected to the high voltage (HV) transformer via a connection at the top of the box; the bottom of the insulator was earthed. The corona discharge was measured using a Rogowski coil on the HV transformer earth bar, with an RC filter to reduce noise. A Clevoscope oscilloscope measured the capacitor voltage of the RC filter, which is proportional to the corona discharge. The applied voltage waveform was measured from the transformer low voltage terminals using the same oscilloscope. The oscilloscope was connected to a computer next to the transformer. A remote desktop connection to a laptop allowed the waveforms to be viewed while working at a safe distance. The intention of measuring the corona discharge was to see how factors such as the amount of ash removed and the type of ash used were reflected in the readings.

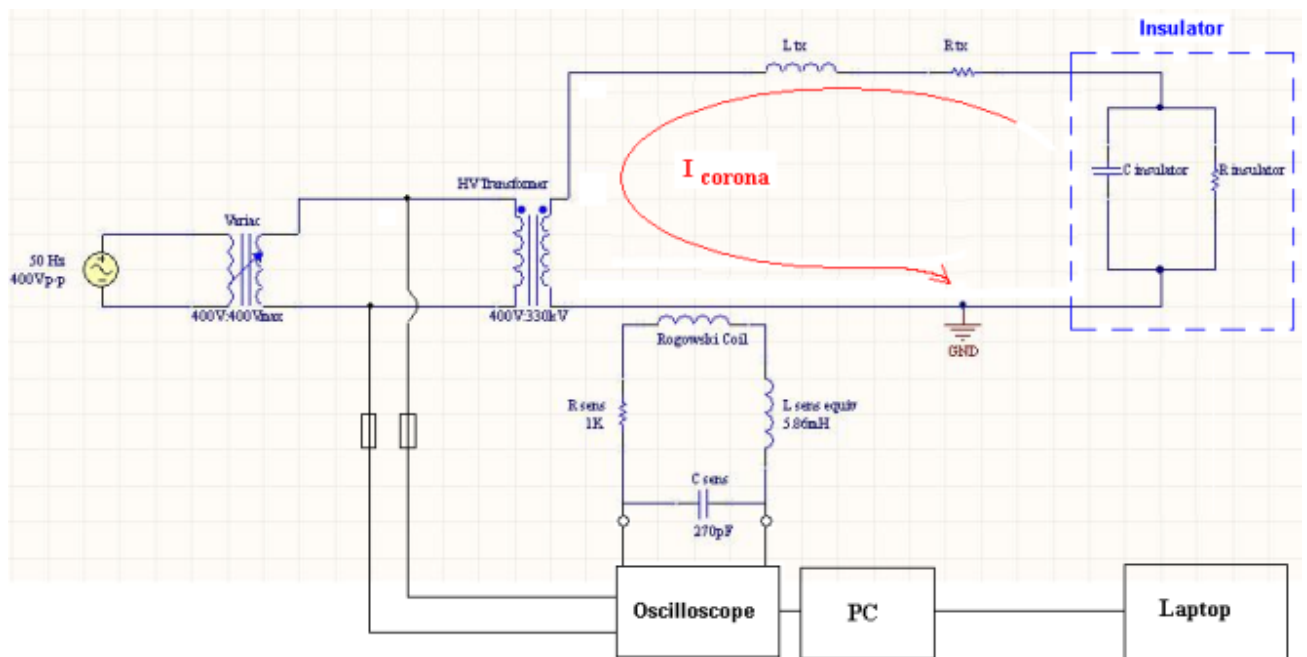


Figure 6: Equipment set-up schematic, including insulator equivalent model and transformer inductance and resistance.

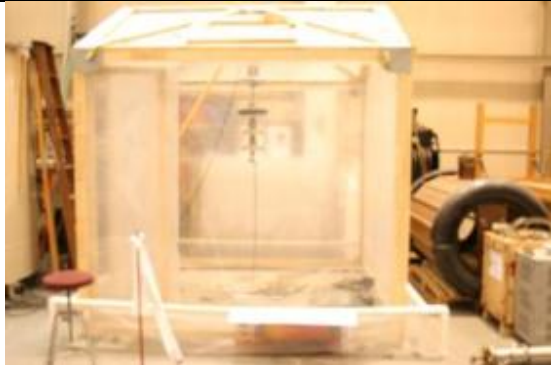


Figure 7: Insulator hanging in a box to contain the ash.



Figure 8: Ash-covered insulator, with grading ring and aluminium tube to reduce unwanted corona on the HV line.

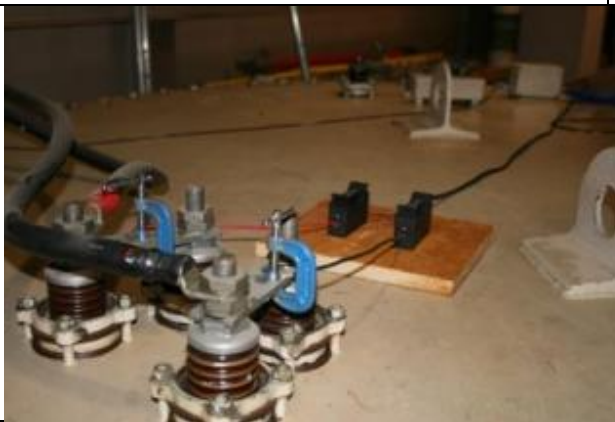


Figure 9: Applied voltage is measured on the low voltage side of the transformer.



Figure 10: Rogowski coil discharge sensor on HV transformer earth bar.



Figure 11: Cleverscope oscilloscope (left of monitor) connected to a PC.



Figure 12: Laptop, sitting next to transformer control panel, with remote desktop connection to oscilloscope PC.



## 4.2 Insulators



Four different insulators of similar lengths were tested: a polymeric, ceramic and two different sized glass insulators – referred to as big and small glass insulators throughout this report. The insulators are shown in Figure 13.

## 4.3 Ash

Three different grain diameters of basaltic pseudo ash were used:  $<0.1\text{mm}$ ,  $<1\text{mm}$ ,  $>1\text{mm}$ . The ash was created in the Department of Geological Sciences, University of Canterbury. Only dry ash was tested.

## 5. RESULTS

### 5.1 Elecnet Models

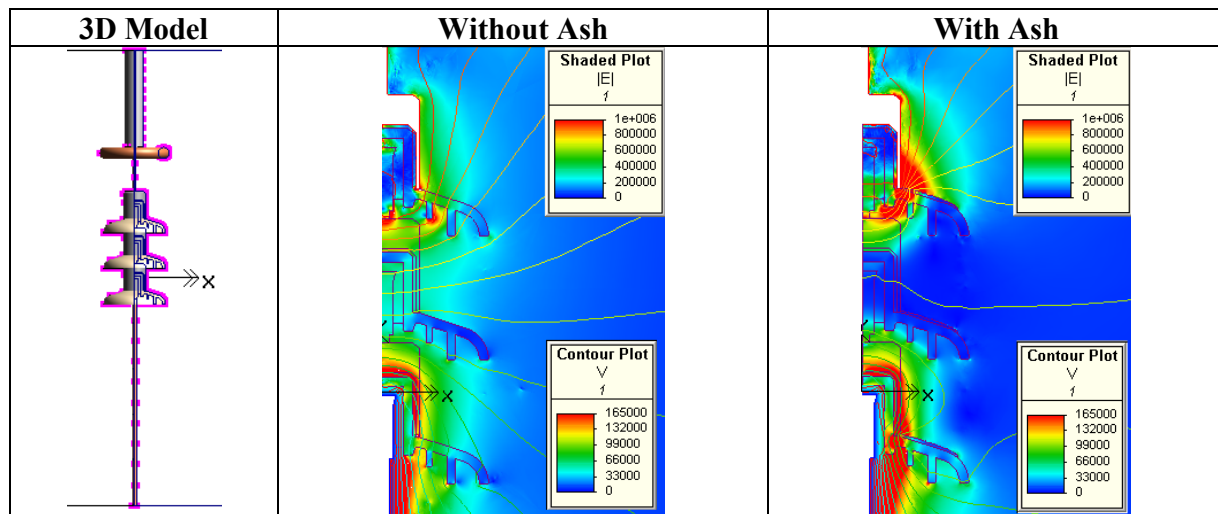


Figure 14: Elecnet model of electric field for (+) 165kV applied voltage (note: 'x' is purely to show the x axis of the model).

Elecnec is a finite element analysis (FEA) program used to model electric fields. A free, two-dimensional version\* of Elecnec was used to create models of the electric field around insulators with and without ash. Figure 14 shows the model constructed for the big glass insulator, the other models are given in appendix 10.1 along with the material parameters used. The red shaded areas of Figure 14 represent strong electric field; the blue shaded areas represent weak electric field. The equipotential lines of Figure 14 are similarly colour coded, where red represents high voltage and blue represents low voltage. The key result from the models is that the electric field

should be strongest on the top and bottom weather sheds, and weak on the middle shed. Therefore, according to the corona wind hypothesis, ash should be removed predominantly from the top and bottom weather sheds, with little removal from the middle weather shed.

## 5.2 Preliminary Experimental Observations

A 2mm to 5mm thick layer of <1mm ash was applied to the four different insulators and 165kV applied for approximately 2 minutes while discharge waveforms were acquired. Photos showing the amount of ash removed are given in Figure 15. The amount of ash removed was similar for the glass and ceramic insulators – ash was predominantly removed from the top weather shed, with a small amount removed from the middle and bottom weather sheds. The maximum amount of ash removed was approximately 90% from the top weather shed and 30% from the middle and bottom weather sheds using the big glass insulator. The polymeric insulator flashed over at 130kV, and only a very small amount of ash was removed from the top weather shed.

\*The free version of Elecnet allows construction of a 3-D model about a single axis of symmetry, but only analyses the field in 2-D.

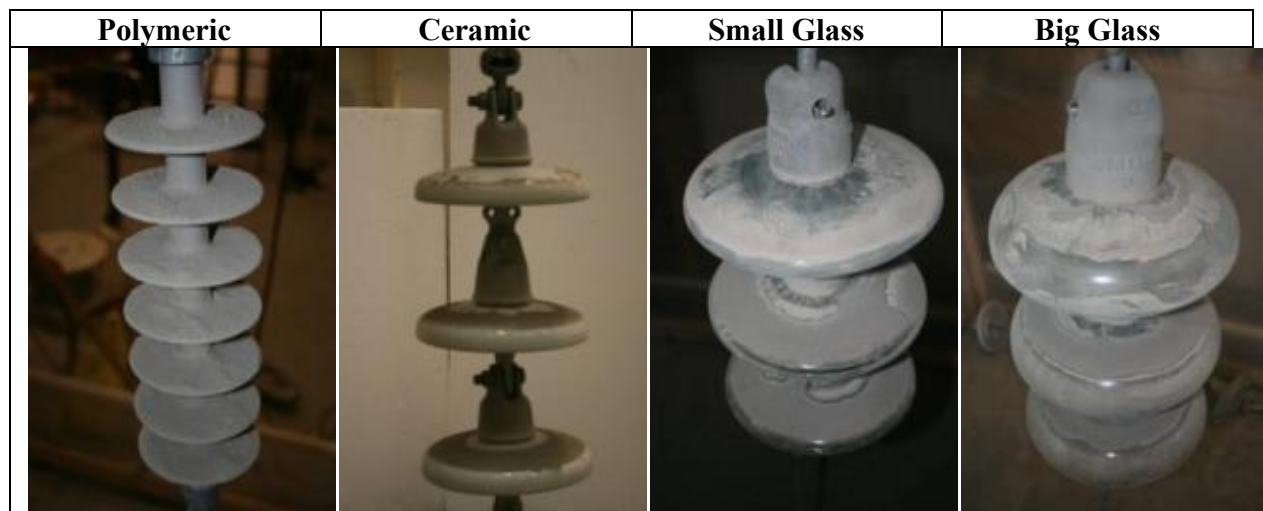


Figure 15: Comparison of ash removed after 2 minutes at 165kV for different insulators.

## 5.3 Detailed Experimental Observations

### 5.3.1 Rapid Photo Sequence

Using the Cannon Eos digital camera set on sport mode, a rapid sequence of photos of ash removal was obtained while the voltage was increase to 165kV and held there for 1 minute. The photos revealed that ash is removed in bands, which start at the outer and inner edges of the weather shed and move towards each other. A segment of the sequence is given in appendix 10.2.



### 5.3.2 High Speed Video Camera

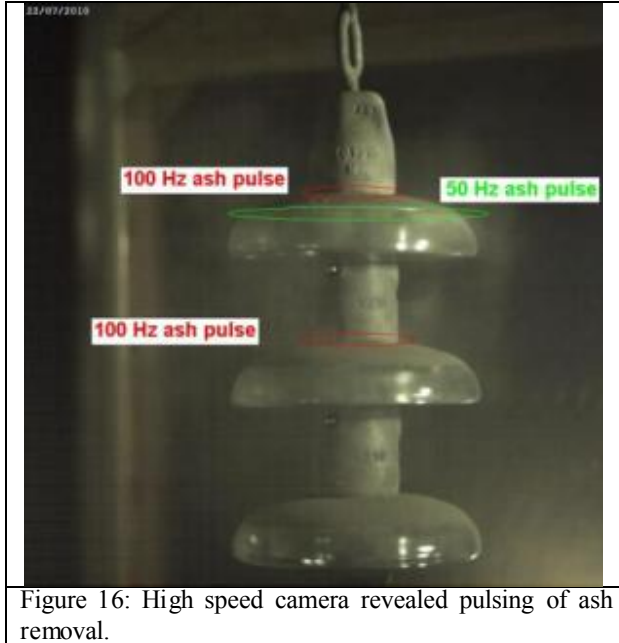


Figure 16: High speed camera revealed pulsing of ash removal.

The Department of Geological Sciences high speed video camera was used to record the ash removal phenomena. The settings used are given in appendix 10.3.

The video showed ash pulsing off the outer edge of the top weather shed at a consistent 50Hz rate. The location of the ash pulses are shown in Figure 16. The ash clouds on the outer edge did not appear turbulent but cleanly dispersed into the surrounding air, mostly away from the high voltage line. Ash also pulsed off the inner edge close to the shaft, but at a less consistent 100 Hz rate, often appearing as a turbulent vertical stream rather than a clean, cloud-like dispersion. The 100Hz pulses appeared to roughly alternate between small and larger pulses.

## 6. DISCUSSION

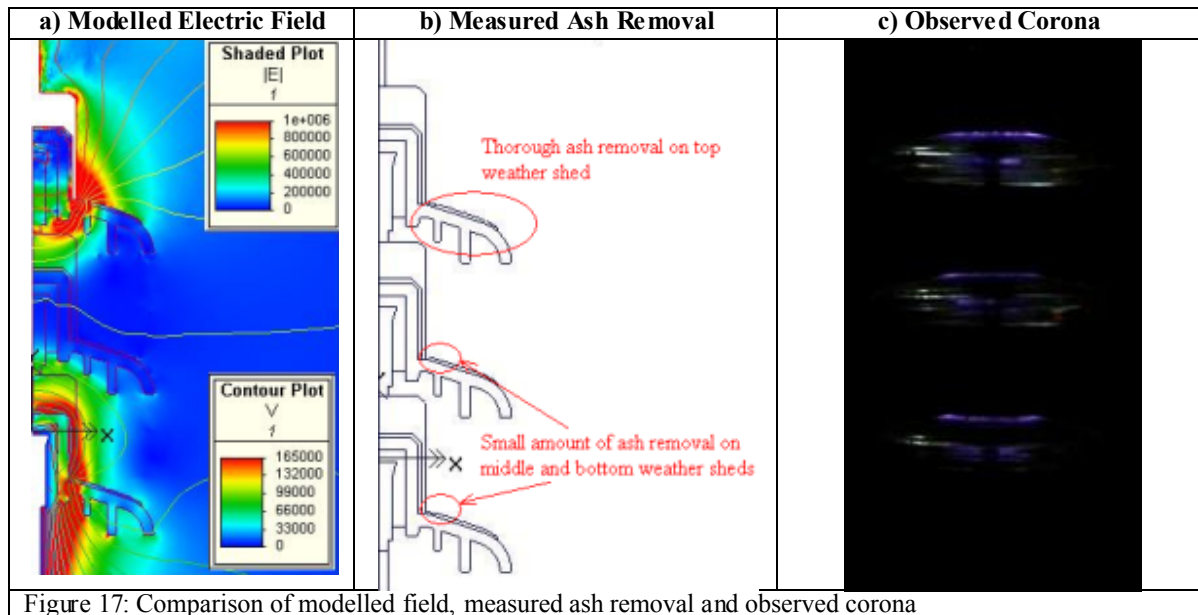


Figure 17: Comparison of modelled field, measured ash removal and observed corona

The models predicted a strong electric field, and therefore strong corona wind and ash removal, mostly on the top and bottom weather sheds, with little ash removal on the middle shed, as shown in Figure 17 a). In reality, ash was thoroughly removed from the top shed with little removal from the middle and bottom sheds, as shown in Figure 17 b). The areas of ash removal and corona coincide, as shown in Figure 17 b) and Figure 17 c), confirming that there is a relationship between the electric field strength and ash removal.

The sequence of photos of ash removal occurring in distinct bands suggests a force more direct than wind. The high speed video of ash pulsing off the insulator surface suggests the ash itself is repelled, and the 50Hz pulsing suggests that there is asymmetry in the electric field strength between half cycles.

Relative permittivity is a measure of the extent to which polar molecules align to reduce electric field strength within a material. As Figure 18 shows, the electric field strength acting on the ash is strongest at the air-ash boundary; therefore, ash is removed from this boundary, creating removal in distinct bands.

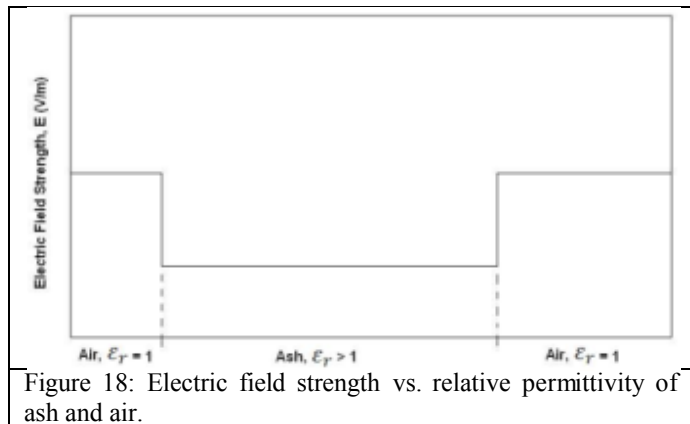


Figure 18: Electric field strength vs. relative permittivity of ash and air.

The corona wind hypothesis relied on the movement of positive ions created by corona discharge. However, calculations given in appendix 10.4 reveal that these positive ions only move a few millimetres during each 50Hz cycle. This creates a build up of positive charge, called space charge, which causes asymmetry in the electric field between half cycles of the 50Hz supply.

Figure 19 demonstrates the electric field asymmetry between positive and negative half cycles caused by space charge, hence explaining the ash pulsing observed. During the negative half cycle, the space charge causes a larger area of strong electric field above the top weather shed due to the proximity of the negative HV line and grading ring to the positive space charge. This results in free electrons gaining more energy, giving more intense electron avalanches and a larger space charge above the top weather shed. It is also possible that more free electrons were available to initiate electron avalanches above the top weather shed, due to effects such as field emission of electrons from the HV components (cable, aluminium tube, grading ring, top insulator cap), which were entirely exposed metal whereas the ground cable was insulated. Field emission requires a very strong electric field in the order of 10M V/m [10] to release electrons from the conductor, which may occur due to irregularities along the conductor surface. The increased corona and space charge resulted in greater ash removal on the top weather shed.

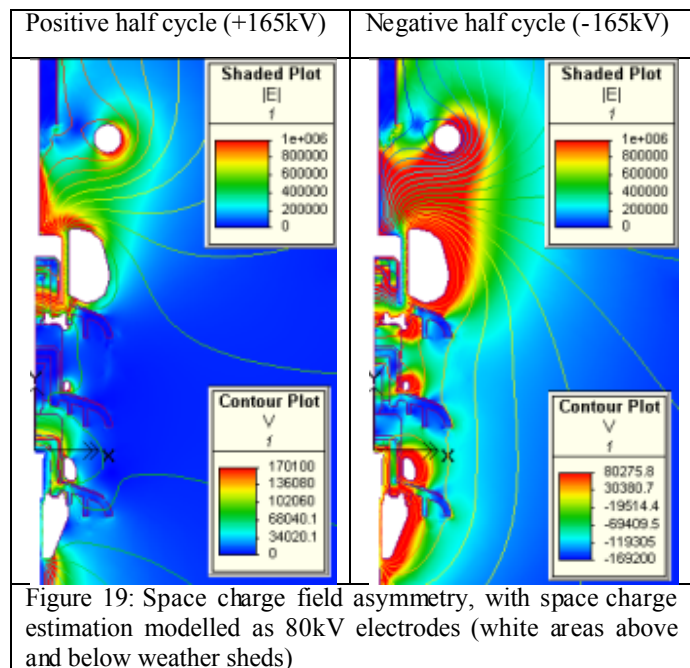


Figure 19: Space charge field asymmetry, with space charge estimation modelled as 80kV electrodes (white areas above and below weather sheds)

It is proposed that leakage currents along the insulator surface and corona discharge allow ash particles to gain a negative charge. The electric field, and therefore force acting on the charged ash, is strongest during the negative half cycle. The direction of the force is upwards, away from the insulator surface due to the positive space charge. Therefore, the ash pulses off the insulator surface during the negative half cycle.



Figure 20: Nylon flock & bitumen create a rough surface which causes corona

Figure 20 shows a rough, black, Velcro-like material present on the glass insulators. This material is a nylon flock glued with bitumen which is required to prevent damage to the glass during assembly. The rough surface creates corona and space charge near the glass-cap junction. The rough, three-dimensional nylon flock could not be modelled with the two-dimensional free version of Elecnet, however an estimation of the resultant space charge is modelled in Figure 19. This space charge gives a region of strong electric field above the middle weather shed which accounts for removal of ash there. The initial models that did not include space charge did not explain ash removal from the middle weather shed.

## 7. FUTURE INVESTIGATION

The theory presented in section 6 relies on two key propositions: the space charge being strongest above the top weather shed, and the ash acquiring a negative charge. These two propositions match the observations made but should be experimentally verified to validate the theory. A comparison of the magnitude and quantity of discharges during positive and negative half cycles of the 50Hz supply waveform may be used to confirm an asymmetry in the electric field. The discharge waveforms acquired were aliased, hence future investigation of the discharge waveforms require an oscilloscope with a faster sampling rate than the 10MHz Cleverscope available during this project.

Many factors such as wind and insulator orientation have been ignored and require investigation to determine whether or not a practical product could be developed. The voltage required to remove the ash is much larger than the normal operating voltage of the insulator, therefore a means of applying a sufficiently high voltage to the power network, or reducing the voltage needed, also requires further investigation. It may be possible to increase the electric field strength and ash removal, for a given voltage, without lowering the flashover voltage by creating an insulator with a decreased direct distance and increased creepage distance.

## 8. CONCLUSIONS

While studying the effect of volcanic ash contamination on high voltage insulator flashover levels, ash was seen 'blowing' off the insulator surface before flashover occurred. The goal of this project was to investigate and explain the observed phenomenon to provide a basis for potential development of self-cleaning insulators.

Areas of ash removal coincided with areas of corona discharge. It was initially proposed that the ash was removed by an AC corona wind however the results do not support this theory. Instead,

the observed results suggest that the ash acquires a negative charge and is removed by an electrostatic force. The electrostatic force is strongest during the negative half cycle of the applied voltage due to space charge and hence the ash pulses off the insulator at 50Hz.

The amount of ash removed increased with the applied voltage and hence electric field, however, this led to a trade off between ash removal and flashover. The maximum amount of ash removed during this project was approximately 90% from the top weather shed and 30% from the middle and bottom weather sheds, using the big glass insulator with 165kV applied for two minutes. This study focused on the removal of dry ash. It is unlikely that wet ash can be removed in this fashion, without flashover, due to the conductive and adhesive nature of wet ash.

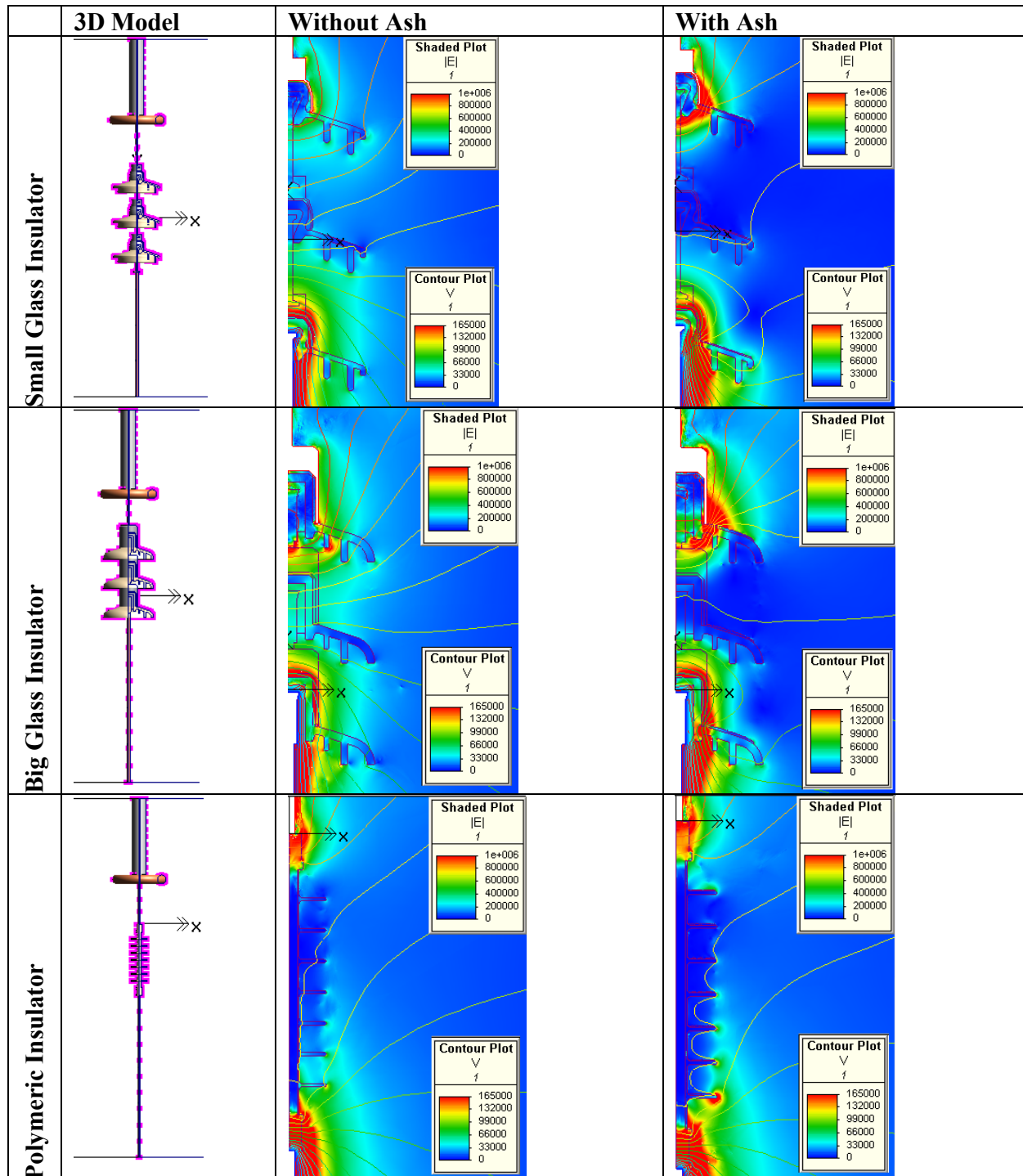
The free, two-dimensional version of Elecnet used to model the electric field did not allow modelling of rough three-dimensional surfaces that are a main source of corona, such as the nylon flock and HV line. Therefore, the initial models created did not agree with the results. By incorporating estimations of the space charge created by the corona, a better representation was obtained. The oscilloscope used did not have a high enough sampling rate to acquire accurate corona discharge waveforms.

## 9. REFERENCES

1. **Sarkinen, C. F.** *Investigation Of Volcanic Ash On Transmission Facilities In The Pacific Northwest*. Vancouver, Washington : Bonneville Power Administration, 1981.
2. **Transpower, Powermark.** *Report on Volcanic Ash Contamination*. Ruapehu : Transpower, Powermark, 1995.
3. **Robinson, Myron.** *A History of the Electric Wind*. New Jersey : Research - Cottrell, Incorporated, Bound Brook, 1961.
4. **Wilson, Jack.** *An Investigation of Ionic Wind Propulsion*. Cleveland, Ohio : NASA, 2009.
5. **David B. Go, Raul A. Maturana, Timothy S. Fisher, Suresh V. Garimella.** *Enhancement of external forced convection by ionic wind*. West Lafayette : School of Mechanical Engineering and Birck Nanotechnology Center, Purdue University, 2008.
6. **Kadete, H.** *Enhancement of Heat Transfer by Corona Wind*. Eindhoven : Eindhoven University of Technology, Faculty of Electrical Engineering, Netherlands, 1987.
7. **N. Balcon, N. Benard, E. Moreau.** *Formation Process of the Electric Wind Produced by a Plasma Actuator*. Poitiers : Laboratoire d'Etudes Aérodynamiques (LEA), Université de Poitiers, ENSMA, CNRS, 2009.
8. **Z. Kucеровsky, W.D. Greason, A. Weigl.** *Corona Wind in a System with the Pin-to-plane*. s.l. : IEEE, 1999.
9. **Moulson, Herbert.** *Electroceramics*. s.l. : Chapman and Hall, 1990.
10. **Kuffel, E.** *High Voltage Engineering Fundamentals*. Oxford : Butterworth-Heinemann, 2000.

## 10. APPENDICES

### 10.1 Elecnet Models



### Material Parameters:

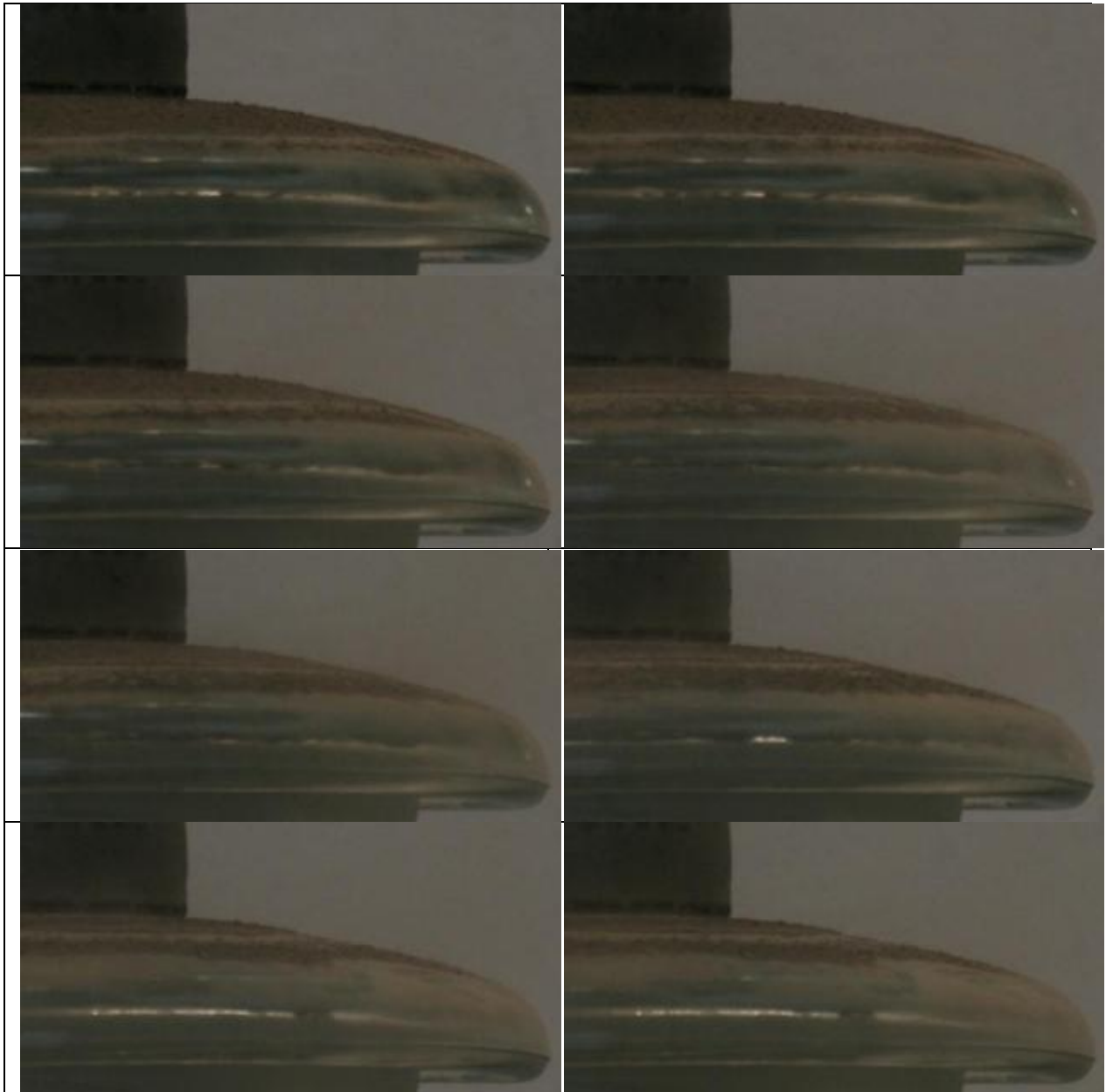
| Material     | Relative Permeability | Coercivity (A/m) | Conductivity (Seimens/m) | Resistivity (Ohm.m) | Relative Permittivity | Thermal Conductivity ( W/(m.C) ) | Thermal Heat Capacity ( J/(kg.C) ) | Mass Density (kg/m3) |
|--------------|-----------------------|------------------|--------------------------|---------------------|-----------------------|----------------------------------|------------------------------------|----------------------|
| Ash          | 1                     | 0                | /                        | 2.00E+07            | 10                    | /                                | /                                  | 1000                 |
| Cast Iron    | 1                     | 0                | 10300000                 | /                   | 1                     | 386                              | 383.1                              | 7200                 |
| Space Charge | 1                     | 0                | 2.50E+07                 | /                   | 1                     | 0.025                            | 1.0056                             | 1.2                  |
| Rubber       | 1                     | 0                | 0.00E+00                 | /                   | 7                     | /                                | /                                  | 1522                 |
| Glass        | 1                     | 0                | 0.00E+00                 | /                   | 5                     | /                                | /                                  | 2000                 |
| Water        | 1                     | 0                | 0.00E+00                 | /                   | 80                    | /                                | /                                  | 1000                 |
| Copper       | 1                     | 0                | 5.77E+07                 | /                   | 1                     | 386                              | 383.1                              | 8954                 |
| Aluminium    | 1                     | 0                | 3.80E+07                 | /                   | 1                     | 204                              | 896                                | 2707                 |
| Air          | 1                     | 0                | 0                        | /                   | 1                     | 0.025                            | 1.0056                             | 1.2                  |

### Approximations:

- Aluminous cement was approximated as aluminium.
- The polymeric insulator weather shed was approximated as rubber.



## 10.2 Rapid Photo Sequence



The sequence (left to right) shows bands of ash removal starting on the outer edge and moving along the weather shed.

### 10.3 High Speed Video Camera Settings

|                |                |
|----------------|----------------|
| Sensor gain    | 0 dB           |
| Rate           | 500 Hz         |
| Exposure       | 329 $\mu s$    |
| Exposure Mode  | Single         |
| Dynamic Range  | 8 Bit          |
| Binning        | 1x1            |
| Pixel Depth    | 24 Bit         |
| ROI            | 1016x1024      |
| Record Mode    | Normal         |
| Frames         | 7937           |
| Recording Time | 15.874 seconds |

## 10.4 Space Charge Analysis: Electron & Ion Movements

|  |  |                  |                     |  |
|--|--|------------------|---------------------|--|
| Description: The maximum distance travelled by a positive ion, for a given electric field strength and frequency, is calculated. |  |                  |                     |  |
| Assumptions:   | 1. Molecules lose 1 electron, hence ions have a charge of 1.692e-19<br>2. Ion direction of travel remains unchanged after collisions<br>3. rms Electric field strength used<br>4. Electric field strength assumed to be the same at all points along the ion path<br>5. Time period of interest = half of 50Hz supply period (=10ms) |                  |                     |  |
| Inputs:  | Value  | Units            | Symbol              |  |
| Assumed kinetic energy maintained by ion after collision with neutral molecule   | 0.50   | Vf/Vinit         | 1/C                 |  |
| Mean free path length  | 1.00E-07   | m                | L                   |  |
| Electric field strength (rms)  | 1.00E+05   | V/m              | E(rms)              |  |
| Elementary charge  | 1.60E-19   | C                | e                   |  |
| Avagadro's Constant  | 6.02E+23   | 1/mol            | N                   |  |
| Frequency  | 5.00E+01   | Hz               | f                   |  |
| Composition of Air:  |  |                  |                     |  |
| Element  | Percentage Composition   | Atomic Number, Z | Mass Number (g/Mol) |  |
| Nitrogen   | 78.090%  | 7                | 14                  |  |
| Oxygen   | 20.950%  | 8                | 16                  |  |
| Argon  | 0.930%   | 18               | 40                  |  |

### Calculated Values:

| Element  | Nucleus/Ion Mass (g) | Electrostatic Acceleration (m/s <sup>2</sup> ) | Mean Time Between Collisions (s) | # Collisions in half period | Distance Travelled (m) | Average Velocity (m/s) | Average Velocity (kph) |
|----------|----------------------|--|----------------------------------|-----------------------------|------------------------|------------------------|------------------------|
| Nitrogen | 2.32E-23             | 6.89E+05                                       | 2.23152E-07                      | 4.48E+04                    | 4.48E-03               | 4.48E-01               | 1.61E+00               |
| Oxygen   | 2.66E-23             | 6.03E+05                                       | 2.3856E-07                       | 4.19E+04                    | 4.19E-03               | 4.19E-01               | 1.51E+00               |
| Argon    | 6.64E-23             | 2.41E+05                                       | 3.77197E-07                      | 2.65E+04                    | 2.65E-03               | 2.65E-01               | 9.54E-01               |
| Electron | 9.11E-31             | 1.76E+13                                       | 4.41716E-11                      | 2.26E+08                    | 2.26E+01               | 2.26E+03               | 8.15E+03               |